IJAME
Int. J. of Applied Mechanics and Engineering, 2025, vol.30, No.1, pp.127-142
DOI: 10.59441/ijame/197489

ANALYTICAL INVESTIGATION OF TAR FOR ENHANCING PERFORMANCE USING VARIED STACK CONFIGURATION AND VARIED WORKING FLUID

K.S Shelke[1], U.S. Wankhede[2], A.K. Yadav[3*] and P. Jurczak[4,5]

[1]Mechanical Engineering, Government College of Engineering Chandrapur, INDIA
[2]Associate Professor, Mechanical Engineering, Government College of Engineering Nagpur, INDIA
[3]Mathematics, Shishu Niketan Model Sr. Sec. School, INDIA
[4]Institute of Mechanical Engineering, University of Zielona Gora, POLAND
[5]Collegium Witelona State University, Legnica, POLAND
E-mail: yadavanand977@gmail.com

Thermoacoustic cooling, which uses sound waves to transfer heat, is an environmentally friendly and simple alternative to conventional refrigeration. Gas mixture adjustment to improve cooling performance is understudied compared to pure gas use. Previous studies focused on pure gas systems, but helium-argon combinations can boost thermoacoustic efficiency. Studying these gas mixtures' synergy could improve cooling efficiency. This study examined different working fluid i.e. pure gas and blend of helium-argon gas to a thermoacoustic refrigerator (TAR) to improve performance. A helium-argon gas mixture's thermoacoustic COP and temperature differential were measured experimentally. The resonator stacks were made of spiral, parallel, and honeycomb with polynamide nylon 6 material. The study focuses on cooling load, frequency, and operating pressure. Our findings suggest that adding helium-argon gas to TARs may improve their performance, broadening refrigeration and cooling applications. Energy was saved by lowering the thermoacoustic activity start temperature using this mixture. The right mix of these gases can outperform pure gas systems, enabling sustained cooling, according to experiments. researchers employ mylar, photographic films, and other stack materials to cool TAR, but 3D printing can create intricate stack structures with polynamide nylon 6. This study highlighted the use of single gas and blend of helium-argon gas mixture to explore polynamide nylon 6 stack materials with varied geometries. The system can be tested with other stack material and different gases at an optimum frequency of *500 Hz*, the cooling performance was observed. The experimental data simulated with the DELTAEC software and observation suggested that a minimum acceptable errors takes place with blended gas mixture and honeycomb stack geometry.

Key words: blend of gas, pure gas, nylon 6, thermoacoustic refrigeration.

1. Introduction

Eco-friendly thermoacoustic cooling employs no toxic refrigerants. Resonators or cooling chambers use sound waves and thermal reactions for thermoacoustic cooling [1]. Gas pressure waves-acoustic waves-drive this. These waves' compression and rarefaction cycles rapidly modify temperature and pressure [2]. To cool, thermal acoustic coolers oscillate. Heat exchangers, stacks, and resonators make up thermoacoustic cooling [3]. Tube or cavity resonators deliver energy to gas mediums by amplifying acoustic waves at certain frequencies. System needs porous or organized resonator stack. Sound waves vibrate gas particles, increasing heat-sound interaction. Rarefaction cools gas particles as they expand at low pressure, while compression heats them [4]. Oscillation cools the stack. Heat exchangers receive and release ambient heat at both stack ends. Geometry, gas type, stack material, and resonator design affect thermoacoustic cooling efficiency [5]. Gas choice impacts sound wave efficiency and speed. Many thermoacoustic devices use argon and helium. The

* To whom correspondence should be addressed

larger molecular weight of argon absorbs and transfers heat better than helium, which propagates sound faster [6]. These gas mixtures boost system performance. Thermoacoustic cooling has numerous advantages over conventional. Without dangerous refrigerants and fewer moving parts, it reduces maintenance and improves system reliability. Thermoacoustic energy optimization reduces energy consumption, notably in heat transfer [7].

Heat transfer by gas particle oscillation in thermoacoustic systems requires the stack. Stack material and shape affect thermal acoustic cooler efficiency [8]. These elements control the system's acoustic-to-thermal conversion and cooling [9]. System efficiency requires stack material to meet thermal, acoustic, and mechanical requirements. Material must have moderate thermal conductivity to sustain stack temperature differential [10]. Too fast or poor heat transmission is inefficient. Material acoustics are important because the stack must transfer sound waves without damping. Porous and high-surface-area materials promote gas particle-stack interaction and heat transmission [11]. Mechanical stability is needed to withstand heating and cooling cycles and acoustic wave pressure changes. To balance thermal conductivity, mechanical strength, and acoustics, nylon 6 is used for stack designs [12]. The stack geometry impacts cooling. Surface area and gas flow differ in parallel plates, cylindrical tubes, and honeycombs. Stack layer spacing (or pores) must be managed for gas particle-stack wall interaction [13]. Ideal spacing matches gas thermal penetration. Stack length, thickness, and cross-sectional area affect cooling as well. Longer stacks enhance temperature gradient and cooling power but increase acoustic losses [14]. Thinner stacks transmit heat but must tolerate pressure variations. Another factor is resonator stack position. Placed where acoustic pressure is strong and gas velocity is modest optimizes gas particle-stack wall contact. Optimization is needed for stack material-geometry interaction. A good material and design that maximizes surface area without constraining gas flow can improve cooling efficiency, whereas a bad setup can hurt it [15]. Stack material and shape determine thermoacoustic cooling system efficiency. Stack design, thermal conductivity, and acoustic transparency maximize heat transmission and cooling. This makes the stack crucial to sophisticated thermoacoustic cooling systems.

Acoustics, cooling, and thermoacoustic cooling system efficiency depend on working gas [16]. Mixing helium and argon cools more. Sound waves compress and rarefy gas in thermal acoustic devices [17]. Gas density, speed of sound, thermal conductivity, specific heat ratio, and temperature oscillations affect heat transfer[18]. Helium transfer acoustic energy by accelerating sound waves. Accelerated temperature oscillations and heat transport increase cooling[19]. Helium absorbs and releases heat during stack oscillations due to its thermal conductivity. Helium with low density decreases viscosity and energy losses, enhancing system efficiency [20]. Argon, along with helium, is important. Dense argon enhances heat absorption, cooling the system [21]. Argon absorbs and stores more heat per volume than helium, favoring heat transmission. Larger temperature gradients cool faster and avoid premature heat dissipation due to moderate thermal conductivity [22]. Best properties of helium and argon increase cooling and acoustics. Argon's heat absorption and helium's quick sound propagation maximize energy and heat transmission [23]. Improve thermoacoustic cooling by changing the helium-argon ratio. Gas balance is difficult due to leaky helium and high cost. Cryogenic cooling, refrigeration, HVAC, and scientific and medical equipment use helium-argon thermal acoustic cooling [24]. Despite the difficulty of adjusting gas composition and managing helium leakage, the mixture's acoustic and thermal properties make it an effective and environmentally friendly way to improve thermoacoustic refrigeration.

Working gases transmit and store acoustic energy, affecting thermoacoustic device performance [25]. Heat-driven thermoacoustic refrigerator operating gas effectiveness must be analyzed. Giacobbe *et al.* estimated gas combination Prandtl values in 1994 to aid choose thermoacoustic refrigerator gases [26]. In 1999, Jin *et al.* studied how mixed gases affect thermoacoustic refrigerator performance using Giacobbe's linear thermoacoustic theory. Their findings showed that low Prandtl numbers and acoustic velocities improve thermoacoustic energy conversion [27, 28].

Tijani [29] found that Reducing Prandtl gases improved thermoacoustic refrigerator performance. Later, Belcher *et al.* [30] studied how specific heat ratio and Prandtl number effect thermoacoustic engine onset temperature. Low specific heat ratio and higher Prandtl number lower these engines' onset temperature. In 2009, He *et al.* [31] reported that helium and nitrogen change pressure amplitude and frequency in solar-powered thermoacoustic engines. In small-scale thermoacoustic Stirling engines, helium is less sensitive to system variables than nitrogen and argon, according to Chen *et al.* [25]. Helium performs better than nitrogen

and argon in large-scale thermoacoustic Stirling engines at *0.4* to *2.6 MPa*, according to Dong *et al.* [32]. A compact thermoacoustic refrigerator with two electroacoustic components and one core is designed by Ramadan *et al.* [33]. Included are technical details, manufacture, and testing. The research explores parameter effects on performance indices. Although non-linear factors cause differences, the DeltaEC design model and prototype work similarly. Chi *et al.* constructed a two-unit room-temperature thermoacoustic refrigerator using medium- and low-grade thermal energy [34]. It resonates well with thin tubes and cavities. These heat-driven thermoacoustic refrigerators have the highest power density ever, *14.95 KW/m*^{3}, a minimum onset temperature of *64°C*, and cooling power from *0.66 kW* to *5.62 kW*. Thermoacoustic cooling involves fewer mechanical parts and no toxic refrigerants. By affecting heat transmission and acoustics, stack materials and shape affect thermoacoustic system efficiency. We don't know how nylon 6 affects stack geometries, especially with helium-argon gas. Looking at how circular, rectangular, and triangular stack shapes effect nylon 6 thermoacoustic system cooling efficiency may increase performance. Research has neglected complex stack geometries and material-specific features like nylon 6 in favor of basic thermoacoustic ideas or gas types or simple stack morphologies. Helium-argon gas and nylon 6 geometries in thermoacoustic cooling systems need further study. Despite advances in thermoacoustics, research gaps remain. Few investigations examined nylon 6 stacking. Nylon 6 provides strong mechanical properties and low heat conductivity, however its geometric shape performance is uncertain. Parallel plates were chosen over cylindrical, triangular, and rectangular stacks, which could interfere with acoustic and thermal transfer. While helium-argon blends are well known, stack designs and cooling gas combinations have not been examined.

Various-shaped nylon 6 stack material is used to test a helium-argon thermoacoustic cooling system. A study examines thermoacoustic cooling with cylindrical, rectangular, and triangular stacks. Total cooling efficiency, temperature reductions, and heat transmission will be assessed. The experiment will test nylon 6's thermal, mechanical, and cooling properties with helium-argon gas. Geometries' cooling efficiency under regulated acoustic and gas mixing will be compared. The investigation will identify nylon 6's ideal helium-argon ratio and geometrical patterns. Optimizing industrial and commercial thermoacoustic stack material, form, and gas composition comes last. To solve these gaps, this work studies thermoacoustic system cooling with nylon 6 stacks of various geometries and helium-argon gas.

2. Experimental setup and procedure specifications

Heat exchanger, resonator, and plate or screen stack make up the Hofler thermoacoustic refrigerator (Fig.1). This thermoacoustic cooling technique is new. The thermoacoustic refrigerator's cylindrical metal tube resonator. Two hermetic ends seal helium or air. This resonator cool thermoacoustically. Heat is exchanged between the working fluid and the resonator's hot and cold ends by the heat exchanger. The heat exchanger regulates system medium temperature. Resonator heat transmission is optimized via plate or screen stacks. Copper plates/screens conduct heat. Complex stack design maximizes heat exchange surface area, boosting system efficiency.

Transducers cause resonator compression and expansion. Resonators generate static waveforms by moving working fluid. Thermoacoustics begins with standing wave compression and expansion. In compression, the high-temperature resonator heat exchanger heats the working fluid. Cooler end of working fluid cools into heat exchanger while expanding. Heat is stored and released via resonator plates/screens, boosting system efficiency.

Hofler's thermoacoustic refrigerator relies on a regenerator and a standing wave in the resonator to cool. This intriguing device could assist many refrigeration and cooling applications. The thermoacoustic refrigerator stack's midsection is shown in Fig.1. This stack is necessary for heat transmission in closed resonator tube inert gas. They use heat exchangers on both stack ends. Copper hollow tubes with *2* and *4 mm* diameters make thermal exchangers. The thermoacoustic refrigerator's tubes efficiently transport heat. Copper mesh with *0.6 mm* thickness and *80%* porosity enhances heat transfer between heat exchangers, maximizing system efficiency. Thermoacoustic refrigerator resonators employ nylon 6. It can replace system elements because to its insulation and ease of production. In this experimentation the Helium argon gas mixed with half-half as a total mixture of working fluid. And only this combination is used for this experimentation.

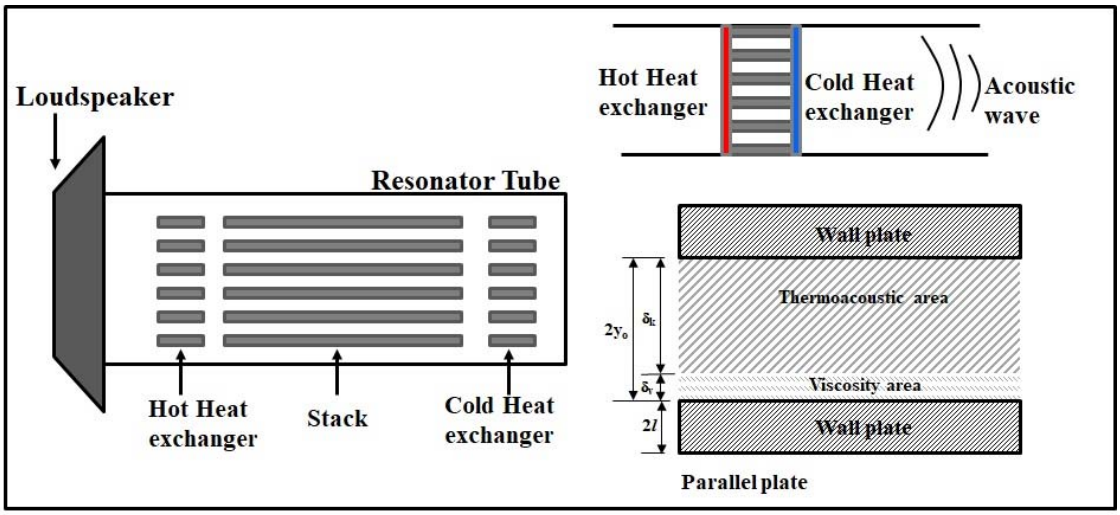

Fig.1. Schematic diagram of a typical thermo-acoustic refrigerator.

Figure 2 shows many essential components of a thermoacoustic refrigerator experimental setup. Heat exchanger, regenerator, driver, resonator, and measurement and control system are incorporated. The system's key resonator hosts the working fluid and generates a stationary acoustic wave. Resonators have metal or ceramic hot and cold ends.

Fig.2. Experimental setup of thermoacoustic refrigerator.

Working fluid leaks are prevented via seals. Heat exchangers are needed for working fluid heat exchange. Most thermoacoustic refrigerators have hot and cold heat exchangers. Copper maximizes heat transfer in these heat exchangers. The regenerator stores and releases thermal energy during resonator

compression and expansion. The regenerator carefully creates a broad thermal conduction surface area on porous media like ceramic or wire mesh. A continuous acoustic wave is generated by the resonator motor. Depending on design, a thermoacoustic refrigerator can use a piezoelectric device, loudspeaker, or mechanical oscillator. The thermoacoustic refrigerator is monitored and controlled. This system measures temperature, pressure, and flow rate with sensors. A computer analyzes and stores data to precisely regulate the thermoacoustic refrigerator's operation.

Speaker assembly (1), flange (2), stack holder (3), resonator tube (4), buffer volume (5), heat exchanger (6), temperature indicator (7), high pressure gauge (8), low pressure gauge (9), are the experimental set. Thermal acoustic refrigeration is popular for its energy- and environmentally-friendly cooling. To maximize system efficiency, stack geometries have been studied extensively. Spiral stacks with honeycomb architecture, circular stacks, and parallel plate stacks have pros and cons. These studies seek the best stack configuration for noise reduction, cooling power, and efficiency. Nylon 6, polycaprolactam, a semi crystalline polyamide. Since it is made by ring-opening polymerization, nylon 6 is unique in the condensation-addition polymer comparison. The elastic, glossy, and durable Nylon 6 fibers are perfect for many applications. They resist wrinkling, acids, alkalis, and abrasion. Nylon 6 glass transitions at *47°C*. Its density is $1.14\ g/cm^3$ and tenacity *6-8.5 gf/D*. It melts at *215°C* and can tolerate *150°C* on average. A perfectly manufactured stack of Nylon 6 sheets was used to study how porosity ratio and gap size affect thermoacoustic refrigeration systems. Figure 3 shows stack arrangements. To evaluate these stacks, we modify drive ratio, mean cooling load, operating pressure, and frequency.

This research shows how porosity ratio and gap size affect thermoacoustic refrigerator performance. Researchers improve thermoacoustic refrigeration systems by understanding these components' physics. Innovative cooling technology can reduce environmental impact and meet the growing need for efficient cooling systems.

a **b** **c**

Fig.3. Various stack geometries spiral, parallel and honeycomb.

To examine how plate spacing impacts thermoacoustic refrigerator performance, particularly temperature differentials, experiments were done utilizing varied operational circumstances and stack geometries. The thermoacoustic refrigerator's resonating system's pressure regulating mechanism altered working pressures from *6* to *10 bar* for these studies. Flexibility makes helium, argon, and their combinations useful. To ensure homogeneity, all experiments were done at *500 Hz*. Thermo-acoustic devices produce temperature gradients with standing waves. Standing waves in common resonator tube dimensions are stable and efficient at *500 Hz*. The system is bulky because lower frequencies require longer resonator tubes, while

higher frequencies can cause acoustic losses and wave propagation inefficiencies. Thermal penetration depth at *500 Hz* matches stack material pore size or spacing. This matching enhances gas-stack heat transfer. At higher frequencies, resonator wall boundary layer viscous losses increase dramatically. Noise under *500 Hz* may be visible and unwanted. Traditional thermoacoustic systems like resonator tubes and stacks are optimized for *500 Hz* frequencies. Compact designs and efficiency are ensured by this frequency. Cold heat exchanger cools using *5A30V DC* power supply unit-powered resistance heating coil. Data collection begins each experimental session after the system stabilizes, maintaining operational pressure. Each experiment evaluates different average cooling load, operating pressure, driving ratio, and frequency to evaluate performance. Controlled and regular experiments provide precise assessment of how plate spacing within the stack impacts thermoacoustic refrigerator performance. These findings could inform thermoacoustic refrigeration system design and optimization for energy-efficient and environmentally friendly cooling. Helium has higher specific heat and thermal conductivity than argon due to its lower molecular weight. Intermolecular interactions make argon denser and have a higher boiling and melting point.

3. Results and discussion

Figure 4 shows the *500 Hz* correlation between cold-end temperature and pressure across stack configurations. Spiral, parallel, and honeycomb architectures have different temperatures, as shown by the graphs. Specific temperature changes are *8-20* degrees Celsius for Spiral, *9-24* degrees Celsius for parallel, and *2-16* degrees Celsius for noneycomb structures.

At 6 *bar* pressure, the parallel structure has the maximum temperature, *28* degrees Celsius. At *10 bar* pressure, the honeycomb structure has the lowest temperature, 2 degrees Celsius. These results illuminate stack configuration performance.

Honeycomb structure leads in temperature control, especially under high pressure. Conversely, the parallel structure achieves higher temperatures, especially at low pressure. These tips help optimize stack configurations for thermoacoustic refrigeration, improving temperature control and system efficiency.

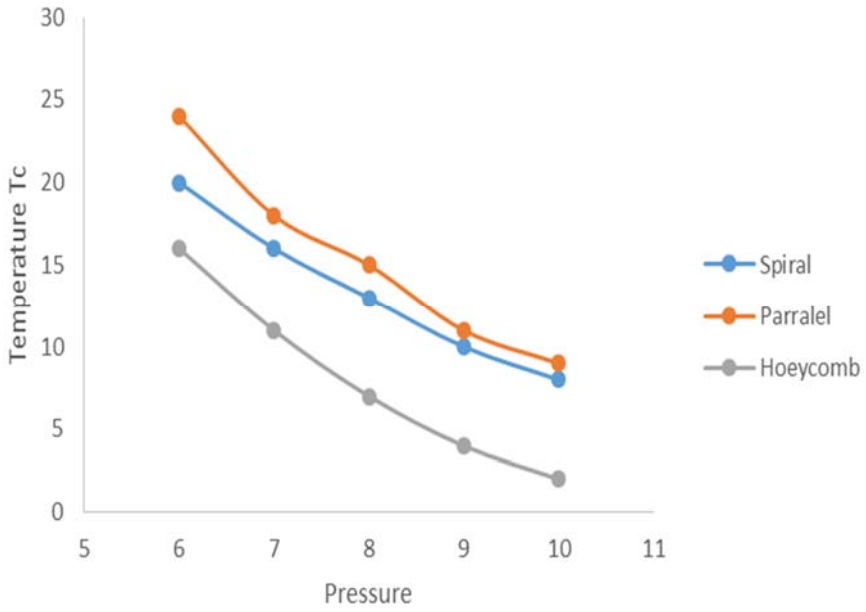

Fig.4. Cold end stack temperature vs pressure at *500 Hz* for diverse stack geometries.

Experimentation data shows that the honeycomb structure performs better with different stack geometries and cooling loads. The honeycomb structure consistently has the lowest cold-end temperatures of all geometries, making it a promising choice for improving thermoacoustic refrigerators.

Figure 5 shows how pressure affects stack's hot end temperature, sustaining a constant frequency and cooling load. The major difference in temperature is around *4* bars in the investigated pressure range. Beyond this limit, raising pressure reduces the temperature difference, showing that air compression doesn't cool. These findings demonstrate that thermally activated refrigerators (TARs) have an ideal pressure range for maximum temperature differentials. Engineers can improve TAR system efficiency and efficacy by identifying the optimal pressure range. These discoveries enlighten the physics of thermoacoustic refrigeration and contribute to its enhancement of performance and design.

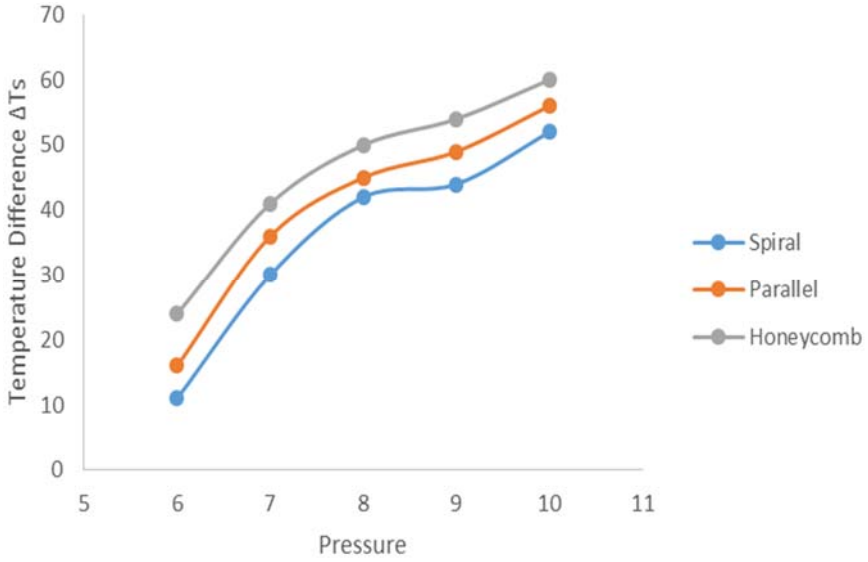

Fig.5. Hot end stack temperature difference vs pressure at *500 Hz* for diverse stack geometries.

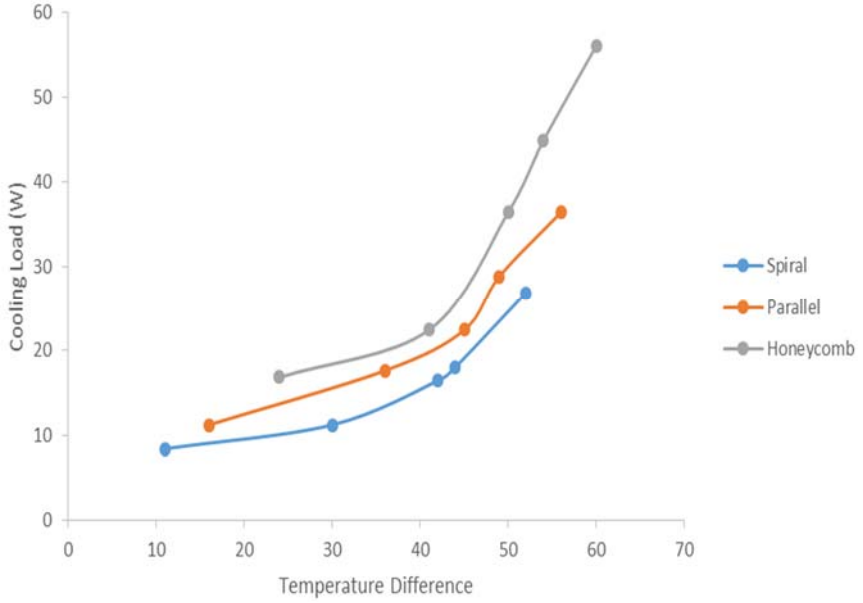

Fig.6. Stack geometry impact on cooling load and temperature difference.

Figure 6 shows how the cooling load and stack temperature differential relate. The graph plainly demonstrates a linear relationship between the temperature gap and cooling load, indicating that the temperature difference across the hot and cold sides of the stack increased correspondingly as the cooling load increases.

Darkened areas of the graph represent cooling load assessment uncertainty. These uncertainties show cooling load measurements and computations' imprecision. Despite these uncertainties, the graph demonstrates a linear cooling load-temperature gap relationship.

These insights are essential for thermoacoustic refrigerator development and use. Cooling load and temperature gap knowledge helps engineers improve system performance. This study exposes thermoacoustic refrigeration fundamentals and may help this burgeoning industry build more accurate and efficient systems.

TAR and charging pressure mean COP are shown in Fig.7. In testing, honeycomb stacks reached *0.498* COP. Charging pressure changes affect the system, as demonstrated by COP fluctuations.

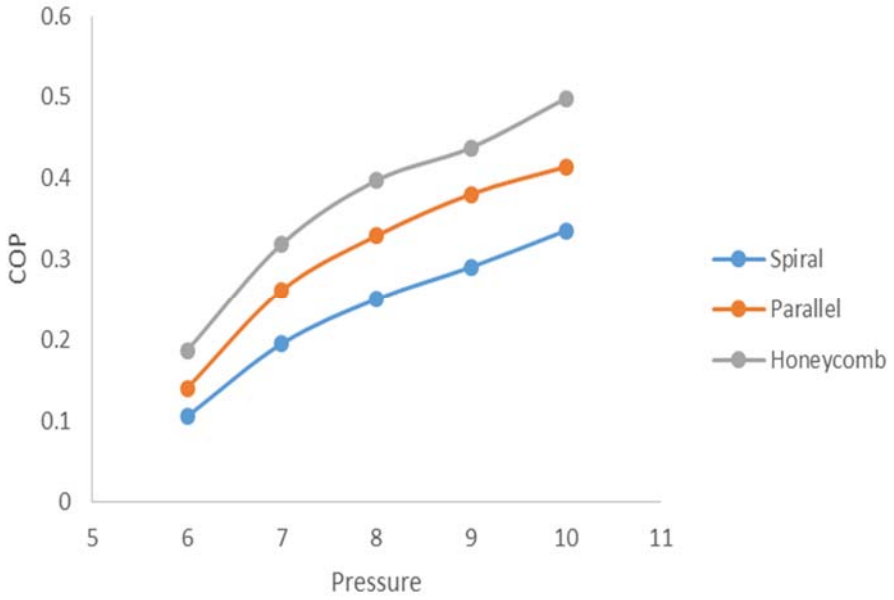

Fig.7. Charging pressure and stack geometry affect COP.

A COP of *0.43* may seem low compared to conventional vapour compression refrigeration systems, but thermoacoustic refrigerators (TARs) have unique performance characteristics and are still in development. Vapour compression devices have lower COPs than thermoacoustic cooling.

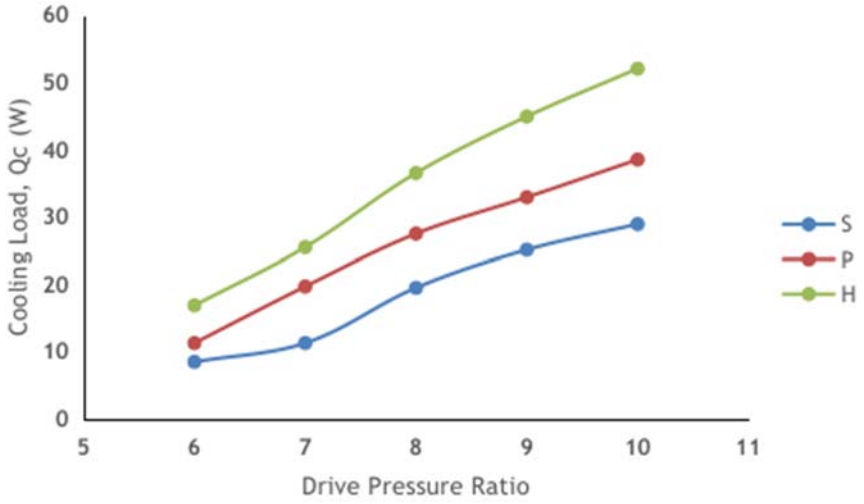

Fig.8. Effect of drive pressure ratio on cooling load of the system, helium-argon as a working fluid.

A thermal absorption refrigeration (TAR) system with a COP of *0.498* can cool efficiently and sustainably. These technologies could become more efficient and commercially viable with more research and development. These findings provide light on TAR performance and opening the path for more eco-friendly and efficient cooling methods.

Figure 8 shows the cooling load grows substantially for all setups as the drive pressure ratio approaches 7. The parallel and spiral stacks climb moderately to *11 W* and *20 W*, respectively, while the honeycomb stack leads with *25 W*. With a slight increase in drive pressure ratio, all designs improve cooling performance dramatically. Between drive pressure ratios *8* and *10*, all configurations' cooling load increases, but slowly. Honeycomb stacks have the largest cooling load, *52 W*, with a drive pressure ratio of *10*. Spiral stack gets *29 W*, parallel stack *38 W*. The honeycomb stack beats the other layouts in cooling capacity, especially at higher pressure ratios. For cooling load capacity across drive pressure ratios, the honeycomb structure is best, especially at higher ratios. At larger ratios, the parallel stack improves and becomes more efficient. Spiral stacks start with the lowest cooling load but improve consistently, reaching comparable results to parallel stacks at greater pressures.

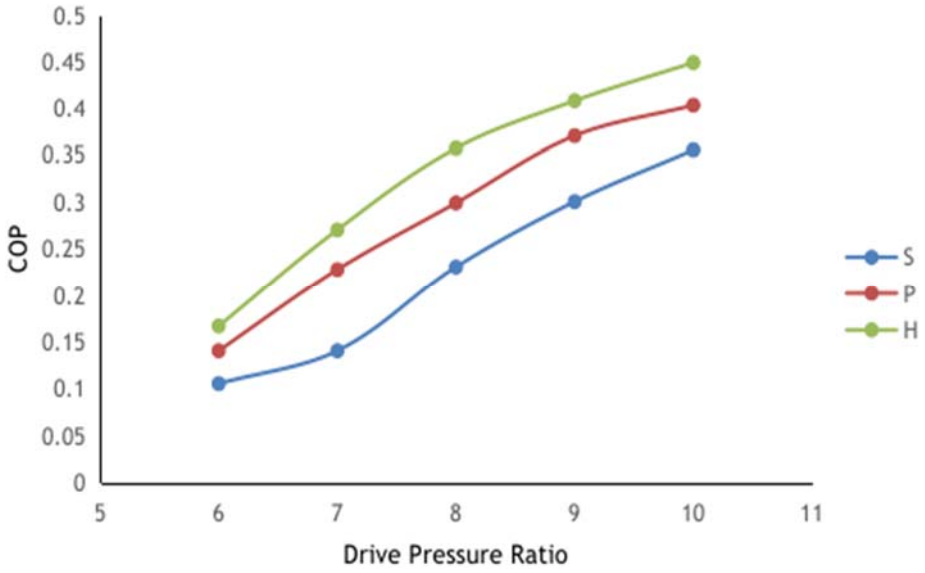

Fig.9. Effect of drive pressure ratio on COP of the system, helium-argon as a working fluid.

Figure 9 shows higher drive pressure ratios improve efficiency in all setups, albeit at different rates. Since the honeycomb stack increases COP the greatest, it may be the best option for high-pressure applications. Although improving, the spiral stack is less efficient than the other variants. The honeycomb stack has a higher COP when helium is employed as the working fluid.

Figure 10 compares cold end temperatures (Tc) for helium (He) and helium-argon (HA) working fluids for spiral, parallel, and honeycomb stack geometries at driving pressure ratios.

Helium-argon (HA) has lower cold end temperatures than helium in all stacks. At *25°C* at a driving pressure ratio of 6, the Spiral design with Helium (S-He) performs intermediately, dropping to *12°C* at *10*. This shows that the S-HA structure is less effective at lowering cold end temperatures than other arrangements, making it less valuable in research.

Honeycomb structure with helium-argon (H-HA) has the lowest temperatures, *16°C* at *6* driving pressure ratio and *2°C* at *10*. Current research requires low cold end temperatures; hence the H-HA configuration's superior cooling is ideal. Categories' greatest temperatures are P-HA and P-He. As pressure ratio increases, both systems cool, but helium-argon stays cooler. Helium-argon (H-HA) honeycombs start at *16°C* at a drive pressure ratio of *6* and drop to *2°C* at *10*. The temperature drop is less significant than H-He but still effective. The cold end temperature is influenced by working fluid and stack layout. Helium-argon has

the lowest temperatures of all combinations, making it more efficient with possible benefits for research that requires lower temperatures. Honeycomb cools best using helium-argon. The proper working fluid and stack structure for the current research's temperature requirements are stressed by this analysis.

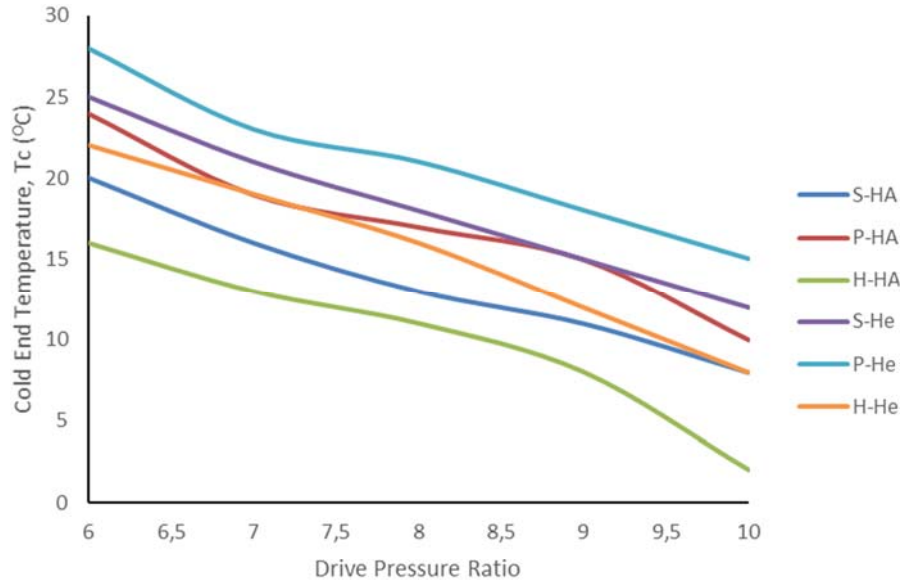

Fig.10. Comparison of cold end temperature of the different stacks geometry for helium and helium-argon gas.

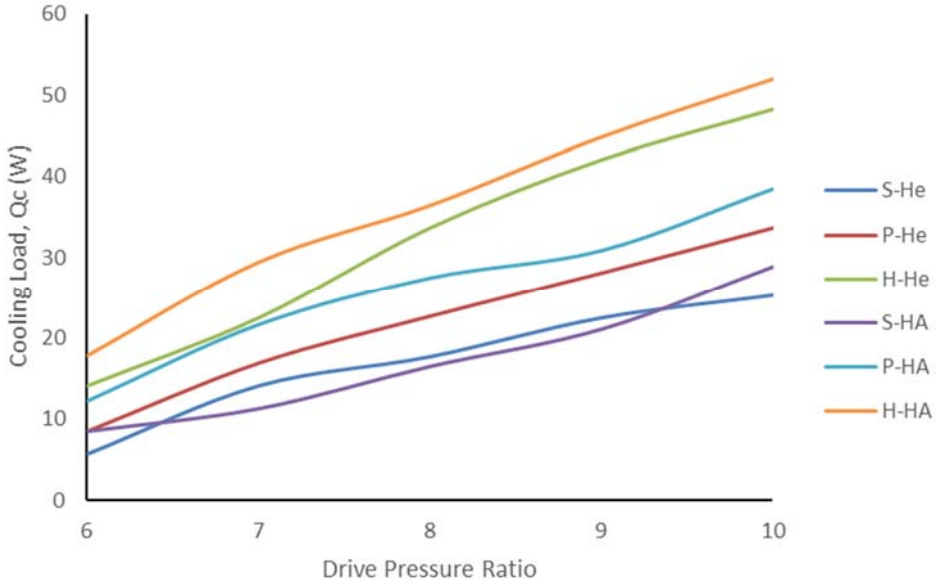

Fig.11 Comparison of cooling load of the different stacks geometry for helium and helium-argon gas.

The cooling load capacity of helium (He) and helium-argon (HA) gases across spiral (S), parallel (P), and honeycomb (H) stack geometries as a function of driving pressure ratio is shown in Fig.11. Cooling load capacity (Qc) in watts (W) is on the *y*-axis, while drive pressure ratio is on the *x*-axis. All geometry helium-argon cooling loads rise with driving pressure ratio. The honeycomb arrangement (H-HA) cools best at *52 W* at *10* drive pressure ratio. Next best is parallel configuration (S-HA), with *40 W*, while spiral configuration (P-HA) is lowest at *29 W*.

Helium-argon mixtures enhance cooling load with higher driving pressure ratios but lower values than pure helium. At *45 W*, honeycomb geometry (H-HA) offers the maximum helium-argon cooling load capacity. Both spiral (S-HA) and parallel (P-HA) layouts peak at *30 W* and *25 W*, respectively. Helium cools better than helium-argon in all stacks. Both gases improve cooling capacity as driving pressure ratio increases, however pure helium surpasses helium-argon. Honeycomb stacks offer the most cooling load, followed by spiral and parallel. This analysis demonstrates that pure helium and honeycomb stacks maximize cooling load.

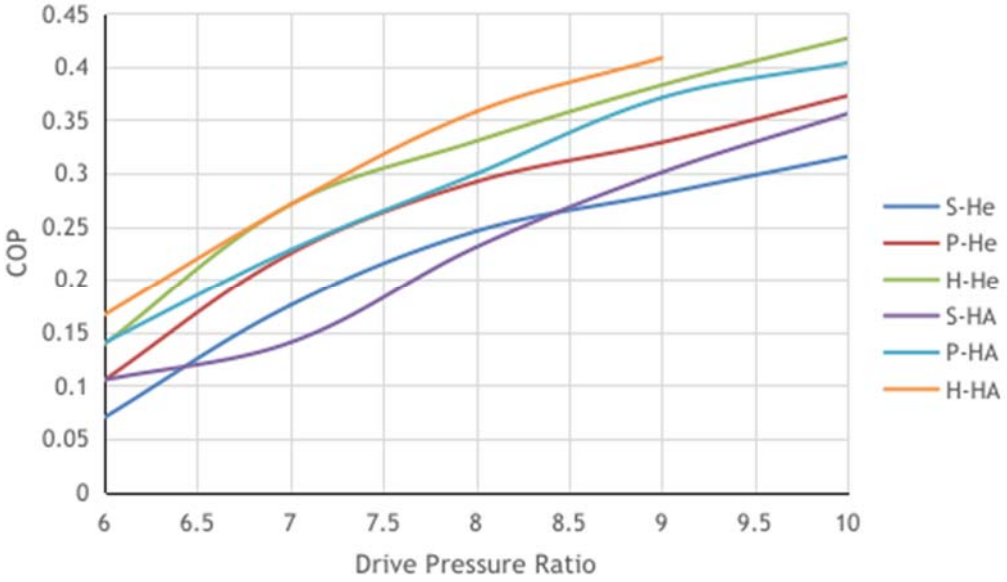

Fig.12. Comparison of COP of the different stacks geometry for helium and helium-argon gas.

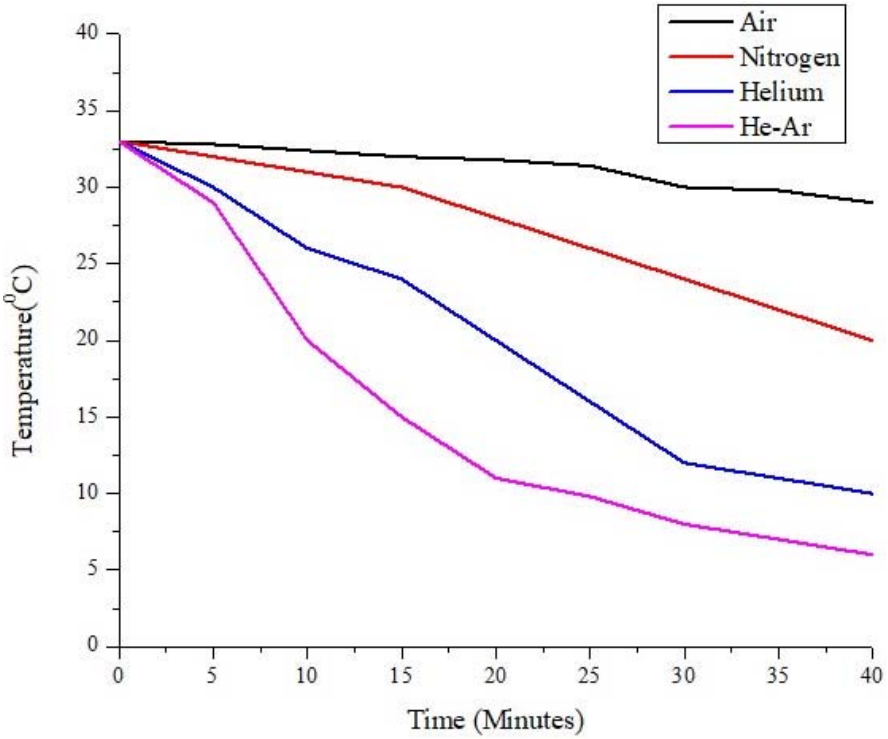

Fig.13. Comparison of varied gas with honeycomb stacks geometry.

Figure 12 shows the coefficient of performance (COP) of helium (He) and helium-argon (HA) gases across spiral (S), parallel (P), and honeycomb (H) stack geometries as a function of driving pressure ratio. The COP on the y-axis measures cooling efficiency, while the drive pressure ratio on the *x*-axis shows system pressure differential. Helium-argon (HA) COP grows gradually with drive pressure ratio in all geometries. The honeycomb arrangement (H-HA) has the maximum efficiency, with COP near *0.43* at *10* driving pressure ratio. The parallel configuration (S-HA) performs next best with a COP of *0.40*, while the spiral configuration (P-HA) performs worst with *0.35*.

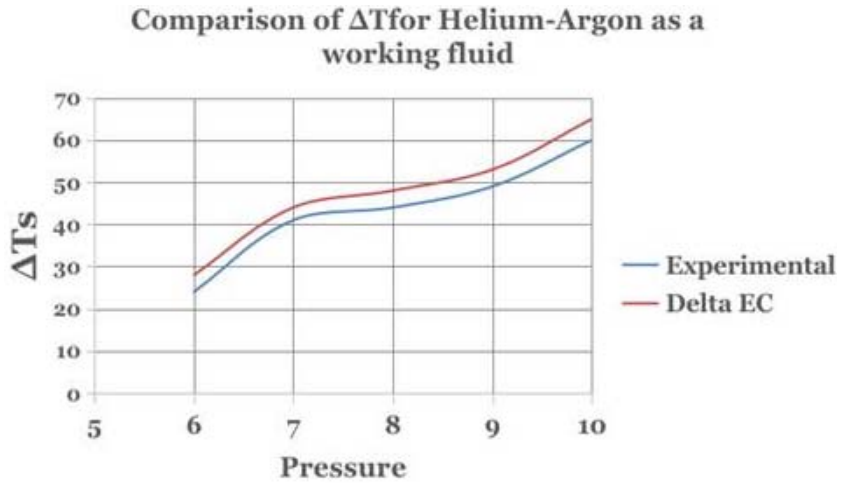

Fig. 13 Simulation of experimental data with DeltaEC software.

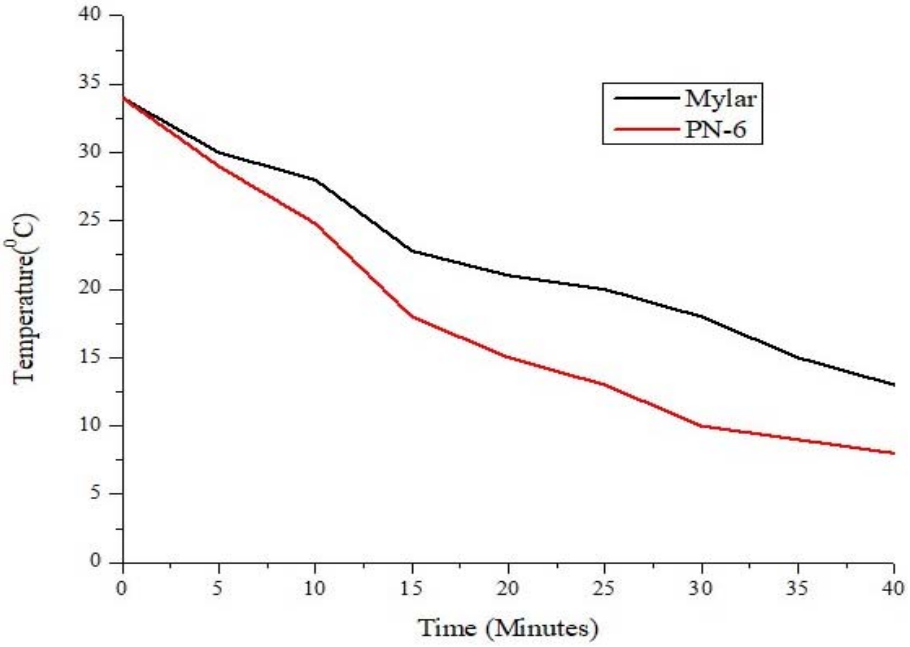

Fig.14. Comparison of varied stack material.

Figure 13 shows the comparative analysis of the honeycomb stack geometry with varied working fluids. As the honeycomb stack geometry shows optimum potential of cooling enhancement in the thermoacoustic refrigeration system, hence the same geometry compared with the various working fluids. The graph plots between the temperature versus time intervals and it shows that the minimum temperature drop

occurs when air was used and the maximum temperature drop occurs when blend of helium-argon gas was used as working fluid, this is because the heat carrying capacity with the inert gases was more as compared to the air or other gases.

Figure 14 shows the comparative analysis of the varied stack material with temperature drop over a period of time. The study compares two stack material viz., mylar and polynamide nylon 6 and the observations concluded that the polynamide nylon 6 gives better results as compared to mylar material.

Fitting model verification into DeltaEC software is tough. Because DeltaEC software only recognizes working model geometry by number. It has a DUCT section but can't draw cylinders or other shapes. Add model to DUCT segment by length, perimeter, and area. Resonators and buffer volumes are easier to fit than stacks and heat exchangers with complex geometry. In BEGIN, loudspeaker output is incorporated, and DeltaEC does not have stack material for test setup, thus mylar is used for validation. The cooling capability sweep was done gradually to compare performance. Test setup dimensions match Tijani's thermoacoustic refrigerator, therefore validations use it. DeltaEC Model considers stack tube and heat exchanger inner diameter. DeltaEC's parallel, square pin-array plates stack. DeltaEC models square honeycomb stacks since the experiment proved they cool better. DeltaEC program shows higher temperature difference without losses than experimental data. Average temperature differential of *8-10%* is accepted in TAR system literature.

Working gas combination greatly affects thermo acoustic refrigeration system COP, which measures efficiency. He-Ar mixture enhances COP for these reasons. Acoustic impedance measures sound wave transmission through working gas. He-Ar mixtures use helium's high-speed sound propagation and argon's higher impedance-matching capabilities to transfer energy between acoustic waves and the working gas. Energy losses are reduced and acoustic energy is converted into thermal energy, enhancing efficiency. Helium's excellent thermal conductivity improves system heat transmission. However, argon's weaker thermal diffusivity minimizes oscillatory thermal energy losses. The combination balances heat transport and energy conservation for effective refrigeration. Light gas helium minimizes viscous losses in oscillating motion, while argon adds bulk to help working fluids interact with the acoustic field. The mixture reduces viscous dissipation, increasing COP. The He-Ar mixture allows working fluid qualities to be adjusted for varied operating situations like temperature ranges or acoustic frequencies, improving performance under diverse loads. The mixture's He-Ar characteristics boost heat transmission, reduce losses, and optimize the system, improving thermo acoustic refrigeration system performance.

4. Conclusion

Results from experiments were better type of thermal acoustic resonance device that uses a fluid mixture of helium and argon as its operating medium. Resistive heating was used to manage the cooling load during testing instead of a cold side heat exchanger.

The research demonstrated a strong correlation between the hot-cold temperature differential and the stack cooling load. Since the cooling load increases with temperature differential, TARs require a wide temperature differential to achieve their cooling efficiency goals. A higher driving pressure ratio and resonance frequency resulted in a higher stack hot end temperature. The temperature differential between the stack and the drive pressure grows in direct proportion to the resonance frequency. Therefore, the ratio of driving pressure to performance coefficient is directly proportional. The study also demonstrated that higher pressure does not always result in higher cooling temperatures and loads. Stack geometry was also a determinant of system efficiency. We need to optimize the stack design to attain the performance we need.

The best COP is *0.498* for honeycomb stack shapes. According to the study's greatest COP, thermoacoustic refrigeration can provide cooling that is both cost-effective and good for the environment.

Our understanding of the performance of TARs fueled by helium and argon is enhanced by this research. The results can be used to develop cooling systems that are more dependable and efficient, which will help satisfy the demand for environmentally friendly and sustainable cooling technology. By gaining a better grasp of the ideal working conditions and mechanics, engineers and researchers may construct TARs that are highly reliable, environmentally friendly, and efficient at cooling. According to the results of the experiments and the software developed by DeltaEC, the thermoacoustic refrigeration system's performance

is enhanced by using honeycomb stack geometry with a gas combination. Research into operational factors, materials, stack designs, working fluids, and cooling load management can enhance thermal energy storage systems. These results have the potential to improve the efficiency and reliability of TARs, making them a sustainable and environmentally beneficial cooling solution.

Acknowledgments

The authors would like to acknowledge the professionalism, enthusiasm and supportive nature of all the faculty members of Government College of Engineering, Chandrapur, Maharashtra, India who supported us for a completion of this research work.

Nomenclature

a – sound velocity of gas $[m/s]$

B – blockage ratio

C_p – specific heat capacity $[J/kg \cdot K]$

D – drive ratio

f – frequency $[Hz]$

K_v – wave number

L – resonator length $[m]$

L_{SN} – normal stack length $[m]$

L_s – length of stack $[m]$

$2l$ – stack plate thickness $[m]$

Pm – average pressure

Po – dynamic pressure amplitude

Q_{cn} – cooling power $[W]$

T_c – cold heat exchanger temperature $[K]$

T_h – hot heat exchanger temperature $[K]$

T_m – mean temperature $[K]$

ΔT_m – temperature gradient

W_n – acoustic power $[W]$

X_N – normal stack position $[m]$

X_s – stack center position $[m]$

x_s – position of the stack $[m]$

$2y_0$ – stack plate spacing $[m]$

β – thermal expansion coefficient $\left[K^{-1}\right]$

γ – ratio, isobaric to isochoric specific heats

δ_k – thermal penetration depth of gas $[m]$

δ_{kn} – normalized thermal penetration depth of gas

δ_v – viscous penetration depth of gas $[m]$

λ – wave length $[m]$

μ – dynamic viscosity $\left[Pa \cdot s\right]$

ν – kinematic viscosity $\left[m^2 / s\right]$

ρ_m – density $\left[kg / m^3\right]$

σ – Prandtl number

ω – angular frequency $\left[rad / s\right]$

References

[1] Ali U., Al-Mufti O. and Janajreh I. (2024): *Harnessing sound waves for sustainable energy: advancements and challenges in thermoacoustic technology*.– Energy Nexus, vol.15, p.100320, DOI: 10.1016/j.nexus.2024.100320.

[2] Sahin M.A., Ali M., Park J. and Destgeer G. (2023): *Fundamentals of acoustic wave generation and propagation*.– in Acoustic Technologies in Biology and Medicine, Wiley, pp.1-36, DOI: 10.1002/9783527841325.ch1.

[3] Hou Z. (2022): *Experimental study on pressure evolution of detonation waves penetrating into water*.– Phys. Fluids, vol.34, No.7, DOI: 10.1063/5.0100446.

[4] Savun-Hekimoğlu B. (2020): *A review on sonochemistry and its environmental applications*.– Acoustics, vol.2, No.4. pp.766-775, DOI: 10.3390/acoustics2040042.

[5] Jadhav P.V., Mehta G.D. and Sakhale C.N. (2024): *Effect of stack geometry and operating frequency on performance of thermoacoustic refrigeration*.– J. Phys. Conf. Ser., vol.2779, No.1, p.012095, DOI: 10.1088/1742-6596/2779/1/012095.

[6] Siva Sakthi M., Swathiga Devi C. and Bogadi S. (2024): *Design and analysis of a thermoacoustic cooling system with two-stack arrangement for different types of stacks BT*.– Advances in Mechanical Engineering and Material Science, Springer Nature Singapore, pp.69-84.

[7] Di Meglio A. and Massarotti N. (2022): *CFD modeling of thermoacoustic energy conversion: a review*.– Energies, vol.15, No.10. DOI: 10.3390/en15103806.

[8] Bouramdane Z., Bah A., Alaoui M. and Martaj N. (2022): *Numerical analysis of thermoacoustically driven thermoacoustic refrigerator with a stack of parallel plates having corrugated surfaces*.– Int. J. Air-Conditioning Refrig., vol.30, No.1, p.1, DOI: 10.1007/s44189-022-00002-8.

[9] Xu J., Luo E. and Hochgreb S. (2021): *A thermoacoustic combined cooling, heating, and power (CCHP) system for waste heat and LNG cold energy recovery*.– Energy, vol.227, p.120341, DOI: 10.1016/j.energy.2021.120341.

[10] Zheng Q., Hao M., Miao R., Schaadt J. and Dames C. (2021): *Advances in thermal conductivity for energy applications: a review*.– Prog. Energy, vol.3, No.1, p.012002, DOI: 10.1088/2516-1083/abd082.

[11] Zhang K. (2021): *The effect of particle arrangement on the direct heat extraction of regular packed bed with numerical simulation*.– Energy, vol.225, p.120244,DOI: 10.1016/j.energy.2021.120244.

[12] Tao Y., Ren M., Zhang H. and Peijs T. (2021): *Recent progress in acoustic materials and noise control strategies - a review*.– Appl. Mater. Today, vol.24, p.101141, DOI: 10.1016/j.apmt.2021.101141.

[13] Da Silva J.D., Moreira D.C. and Ribatski G. (2021): *An overview on the role of wettability and wickability as a tool for enhancing pool boiling heat transfer*.– Advances in Heat Transfer, vol.53, pp.187-248. DOI: 10.1016/bs.aiht.2021.06.003.

[14] Kayes M.I. and Rahman M.A. (2023): *Experimental investigation of a modified parallel stack for wet thermoacoustic engine to improve performance and suppress harmonics*.– Appl. Acoust., vol.212, p.109569, DOI: 10.1016/j.apacoust.2023.109569.

[15] Gassar A.A.A., Koo C., Kim T.W. and Cha S.H. (2021): *Performance optimization studies on heating, cooling and lighting energy systems of buildings during the design stage: a review*.– Sustainability, vol.13, No.17, p.9815, DOI: 10.3390/su13179815.

[16] Xiao L. (2024): *A highly efficient heat-driven thermoacoustic cooling system*.– Cell Reports Phys. Sci., vol.5, No.2, DOI: 10.1016/j.xcrp.2024.101815.

[17] Griffin J.M., Jones S., Perumal B. and Perrin C. (2023): *Investigating the detection capability of acoustic emission monitoring to identify imperfections produced by the metal active gas (MAG) welding process*.– Acoustics, vol.5, No.3. pp.714-745, DOI: 10.3390/acoustics5030043.

[18] Di Meglio A., Di Giulio E., Dragonetti R. and Massarotti N. (2021): *Analysis of heat capacity ratio on porous media in oscillating flow*.– Int. J. Heat Mass Transf., vol.179, p.121724, DOI:10.1016/j.ijheatmasstransfer.2021.121724.

[19] Eanest Jebasingh B. and Valan Arasu A. (2020): *A detailed review on heat transfer rate, supercooling, thermal stability and reliability of nanoparticle dispersed organic phase change material for low-temperature applications*.– Mater. Today Energy, vol.16, p.100408, DOI:10.1016/j.mtener.2020.100408.

[20] Ghorbani B. and Amidpour M. (2021): *Energy, exergy, and sensitivity analyses of a new integrated system for generation of liquid methanol, liquefied natural gas, and crude helium using organic Rankine cycle, and solar collectors*.– J. Therm. Anal. Calorim., vol.145, No.3, pp.1485-1508, DOI: 10.1007/s10973-021-10659-9.

[21] Zhang R., Zhang X., Qing S., Luo Z. and Liu Y. (2023): *Investigation of nanoparticles shape that influence the thermal conductivity and viscosity in argon-based nanofluids: a molecular dynamics simulation*.– Int. J. Heat Mass Transf., vol.207, p.124031, DOI: 10.1016/j.ijheatmasstransfer.2023.124031.

[22] He Z., Yan Y. and Zhang Z. (2021): *Thermal management and temperature uniformity enhancement of electronic devices by micro heat sinks: a review*.– Energy, vol.216, p.119223, DOI:10.1016/j.energy.2020.119223.

[23] Mohebbifar M. R. (2021): *Optical measurement of gas vibrational-translational relaxation time with high accuracy by the laser photo-acoustic set-up*.– Microchem. J., vol.164, p.106040, DOI:10.1016/j.microc.2021.106040.

[24] Ismail M., Yebiyo M. and Chaer I. (2021): *A review of recent advances in emerging alternative heating and cooling technologies*.– Energies, vol.14, No.2. DOI: 10.3390/en14020502.

[25] Chen M. and Ju Y.L. (2015): *Effect of different working gases on the performance of a small thermoacoustic Stirling engine*.– Int. J. Refrig., vol.51, pp.41-51, DOI: 10.1016/j.ijrefrig.2014.12.006.

[26] Giacobbe F.W. (1994): *Estimation of Prandtl numbers in binary mixtures of helium and other noble gases*.– J. Acoust. Soc. Am., vol.96, No.6, pp.3568-3580, DOI: 10.1121/1.410615.

[27] Swift G.W. (2017): *Thermoacoustics: A Unifying Perspective for Some Engines and Refrigerators*.– Springer,

[28] Swift G.W. (1988): *Thermoacoustic engines*.– J. Acoust. Soc. Am., vol.84, No.4, pp.1145-1180, DOI: 10.1121/1.396617.

[29] Tijani M.E.H., Zeegers J.C.H. and De Waele A.T.A.M. (2002): *Prandtl number and thermoacoustic refrigerators*.– J. Acoust. Soc. Am., vol.112, No.1, pp.134-143, DOI: 10.1121/1.1489451.

[30] Belcher J.R., Slaton W.V., Raspet R., Bass H.E. and Lightfoot J. (1999): *Working gases in thermoacoustic engines*.– J. Acoust. Soc. Am., vol.105, No.5, pp.2677-2684, DOI: 10.1121/1.426884.

[31] Shen C., He Y., Li Y., Ke H., Zhang D. and Liu Y. (2009): *Performance of solar powered thermoacoustic engine at different tilted angles*.– Appl. Therm. Eng., vol.29, No.13, pp.2745-2756, DOI: 10.1016/j.applthermaleng.2009.01.008.

[32] Dong S., Shen G., Xu M., Zhang S. and An L. (2019): *The effect of working fluid on the performance of a large-scale thermoacoustic Stirling engine*.– Energy, vol.181, pp.378-386, DOI:10.1016/j.energy.2019.05.142.

[33] Ramadan I.A., Bailliet H., Poignand G. and Gardner D. (2021): *Design, manufacturing and testing of a compact thermoacoustic refrigerator*.– Appl. Therm. Eng., vol.189, p.116705,

[34] Chi J. (2023): *Numerical and experimental investigation on a novel heat-driven thermoacoustic refrigerator for room-temperature cooling*.– Appl. Therm. Eng., vol.218, p.119330, DOI:10.1016/j.applthermaleng.2022.119330.

Received: October 28, 2024
Revised: December 17, 2024